that the autoclave was free from catalytically active metal impurities.

Acknowledgment.

This work was supported by the National Science Foundation Grant NSF CHE78-09443. Use of the Stanford Magnetic Laboratory NSF Grant GP23633 is also acknowledged.

Registry No. Polybutadiene, 9003-17-2; poly(vinylbenzyl chloride), 9080-67-5; styrene, 100-42-5; α-methylstyrene, 98-83-9; poly(α-methylstyrene), 25014-31-7; benzene, 71-43-2; toluene, 108-88-3; cumene, 98-82-8; $PhCH_2Cl$, 100-44-7; $PhNO_2$, 98-95-3; Pd, 7440-05-3; Rh, 7440-16-6; Ni, 7440-02-0; Co, 7440-48-4; $RhCl(PPh_3)_3$, 14694-95-2; $[Rh(NBD)(PPh_3)_2][ClO_4]$, 32799-31-8; $[Ir(COD)P(i\text{-}Pr)_3py][PF_6]$, 64536-74-9; $[Rh(C_5Me_5)Cl_2]_2$, 12354-85-7.

Thiocyanate Cleaves the Imidazolate-Bridged Dicopper(II) Center in a Binucleating Macrocycle To Form $[Cu_2(SCN)_4 \subset A']$. Model Chemistry for Superoxide Dismutase

Andrea E. Martin[1a] and Stephen J. Lippard*[1a,b]

Contribution from the Department of Chemistry, Massachusetts Institute of Technology, Cambridge, Massachusetts 02139, and Columbia University, New York, New York 10027.
Received August 31, 1983

Abstract: When excess potassium thiocyanate is added to an aqueous solution of $[Cu_2(im) \subset A']^{3+}$ (imH = imidazole; A′ = 1,4,7,13,16,19-hexaazacyclotetracosane) the imidazolate bridge cleaves, as judged by frozen solution electron spin resonance (ESR) spectroscopic measurements and structural studies of the isolated reaction product, $[Cu_2(NCS)_4 \subset A']$. This chemistry parallels that of the four-copper form of bovine erythrocyte superoxide dismutase, Cu_2Cu_2SOD, which shows similar changes in its ESR spectrum upon addition of thiocyanate ion. X-ray crystallographic study of the product reveals the two copper centers in macrocycle A′ to have distorted square-pyramidal geometry, with three ligand nitrogen atoms and one thiocyanate nitrogen donor in the basal plane (Cu–N distances, 1.93–2.07 Å). The apical site of one copper center is occupied by a thiocyanate nitrogen atom (Cu–N = 2.240 (6) Å) whereas the other copper has a weakly coordinated sulfur atom (Cu–S, 2.733 (2) Å) in the apical position. There is no longer a bridge between the two copper atoms, which are 7.577 (1) Å apart. These results demonstrate the value of $[Cu_2(im) \subset A']^{3+}$ as a model for Cu_2Cu_2SOD and imply that, at least in its reaction with thiocyanate ion, the chemistry of the four-copper form of the protein is controlled by the fundamental coordination chemistry of the bimetallic site rather than by properties unique to a protein environment. The compound $[Cu_2(NCS)_4 \subset A']$ crystallizes in the monoclinic system, space group $P2_1/c$, with a = 14.718 (1) Å, b = 14.472 (2) Å, c = 16.569 (1) Å, β = 113.98 (1)°, and Z = 4.

The study of low molecular weight transition-metal complexes is frequently of value in elucidating aspects of the chemistry of metalloproteins.[2] Recently we have prepared and examined imidazolate-bridged dicopper(II) complexes as models[3] for the active site of the 4-Cu form of bovine erythrocyte superoxide dismutase, Cu_2Cu_2SOD.[4,5] The native enzyme, Cu_2Zn_2SOD, is comprised of two identical subunits, each of which contains a histidine (imidazolate)-bridged Cu(II)–Zn(II) active site. These active sites are well separated from one another. In Cu_2Cu_2SOD, the subunits contain fully active imidazolate-bridged bimetallic centers in which Cu(II) has replaced Zn(II). In order to stabilize the imidazolate (imH = imidazole) bridge with respect to hydrolysis in the model compounds,[6] the $[Cu_2(im)]^{3+}$ unit was incorporated into the binucleating macrocyclic ligands A and A′.[7]

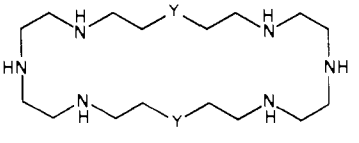

macrocycles A (Y = O), A′ (Y = CH_2)

The complex $[Cu_2(im) \subset A']^{3+}$ (**1**) has several features in common with the Cu_2Cu_2SOD subunits and can be regarded as an excellent model for many of the physical properties of the protein active site.[3,7b,8] Although the superoxide dimustase activity of this complex is difficult to test,[9,10] other biologically relevant aspects of its chemistry can be examined.

Previously we used ESR spectroscopy to show that treatment of Cu_2Cu_2SOD with excess thiocyanate disrupted the magnetic coupling between the copper(II) pairs, a result attributed to cleavage of the imidazolate bridge.[5] The thiocyanate adduct was active as a superoxide dismutase, having more than 50% of the enzymatic activity of untreated Cu_2Cu_2SOD by the 6-hydroxydopamine assay.[5] These results implied that the histidine bridge is not essential for enzymatic activity and therefore need not be invoked in the enzyme mechanism. The purpose of the present investigation was to provide support for these interpretations by examining the reaction of thiocyanate ion with the model compound **1**. In particular, we wanted to learn whether or not the $[Cu_2(im)]^{3+}$ unit remained intact in the presence of excess thiocyanate and what the structure of the resulting adduct would be. Here we present the results of ESR spectroscopic and X-ray crystallographic studies demonstrating that excess thiocyanate

* Address correspondence to this author at M.I.T.

(1) (a) Columbia University. (b) Massachusetts Institute of Technology.
(2) Ibers, J. A.; Holm, R. H. *Science (Washington, D.C.)* **1980**, *209*, 223.
(3) Strothkamp, K. G.; Lippard, S. J. *Acc. Chem. Res.* **1982**, *10*, 318.
(4) Fee, J. A.; Briggs, R. G. *Biochim. Biophys. Acta* **1975**, *400*, 439.
(5) Strothkamp, K. G.; Lippard, S. J. *Biochemistry* **1981**, *20*, 7488.
(6) (a) O'Young, C. L.; Dewan, J. C.; Lilienthal, H. R.; Lippard, S. J. *J. Am. Chem. Soc.* **1978**, *100*, 7291. (b) Kolks, G.; Frihart, C. R.; Coughlin, P. K.; Lippard, S. J. *Inorg. Chem.* **1981**, *20*, 2933.
(7) (a) Coughlin, P. K.; Dewan, J. C.; Lippard, S. J.; Watanabe, E-i.; Lehn, J.-M. *J. Am. Chem. Soc.* **1979**, *101*, 265. (b) Coughlin, P. K.; Lippard, S. J.; Martin, A. E.; Bulkowski, J. E. *Ibid.* **1980**, *102*, 7616.
(8) (a) Coughlin, P. K.; Martin, A. E.; Dewan, J. C.; Watanabe, E.-i.; Bulkowski, J. M.; Lehn, J.-M.; Lippard, S. J. *Inorg. Chem.* **1984**, *23*, 1004. (b) Coughlin, P. K.; Lippard, S. J. *Ibid.* **1984**, *23*, in press.
(9) These assays usually require EDTA to suppress the activity of free copper, which is quite an active superoxide dismutase;[10] EDTA extracts copper from $[Cu_2(im) \subset A']^{3+}$.
(10) See, for example: Misra, H. P.; Fridovich, I. *J. Biol. Chem.* **1972**, *247*, 3170.

0002-7863/84/1506-2579$01.50/0

Table I. Experimental Details of the X-ray Diffraction Study of $[Cu_2 \subset A'(NCS)_4]$ (2)

(A) Crystal Parameters[a] at 24 °C			
a, Å	14.718 (1)	space group	$P2_1/c$
b, Å	14.472 (2)	Z	4
c, Å	16.569 (1)	ρ(calcd), g cm^{-3}	1.446
β, deg	113.98 (1)	ρ(obsd),[b] g cm^{-3}	1.465 (5)
V, Å^3	3224.6	mol wt	702
(B) Measurement of Intensity Data[c]			
instrument: Enraf-Nonius CAD-4F κ-geometry diffractometer			
radiation: Mo Kα (λ_{α_1} = 0.70930 Å, $\lambda_{\bar{\alpha}}$ = 0.71073 Å) graphite monochromatized			
standards, measured every 1 h of X-ray exposure time	$(\bar{4}\bar{6}2)$ $(\bar{9}\bar{4}7)$ $(\bar{1}2\bar{9})$		
no. of reflections collected exclusive of systematic absences	6457; [$3 \leq 2\theta \leq 50°$ ($\pm h, +k, +l$)]		
(C) Treatment of Intensity Data[d,e]			
no. of reflection after averaging	6151		
observed unique data $F_o > 4\sigma(F_o)$[e]	4074		

[a] From a least-squares fit of the setting angles of 25 reflections with $2\theta > 30°$. [b] By neutral buoyancy in a mixture of CH_2Cl_2 and $CHCl_3$. [c] See Silverman et al. (Silverman, L. D.; Dewan, J. C.; Giandomenico, C. M.; Lippard, S. J. *Inorg. Chem.* **1980**, *19*, 3379) for typical data collection and reduction procedures employed in our laboratory. [d] No absorption correction was applied. The estimated range of transmission factors was 0.58–0.69. [e] F_o and $\sigma(F_o)$ were corrected for background, attenuator, and Lorentz-polarization of X-radiation as described in the reference of footnote *c*.

cleaves the imidazolate bridge in **1**, which strongly supports conclusions previously reached for Cu_2Cu_2SOD.

Experimental Section

The ligand A′ [1,4,7,13,16,19-hexaazacyclotetracosane)[11] and the complex $[Cu_2(im)\subset A'](ClO_4)_3 \cdot H_2O$[7,8] were prepared as previously described. All chemicals were reagent grade or better and not further purified. Microchemical analyses were performed by Galbraith Laboratories, Knoxville, TN. Electron spin resonance (ESR) spectra were obtained with a Varian E-Line X-band spectrometer equipped with a temperature controller. Spectra were obtained at 140 K. Calibration of the magnetic field was accomplished by using Mn(II), a naturally occurring impurity in strontium oxide.[12] Ultraviolet and visible spectra were recorded on a Cary 118C spectrophotometer. A Perkin-Elmer 621 spectrometer was used to acquire infrared spectra.

Preparation of $[Cu_2(NCS)_4\subset A']$ (2). Method 1 (from $[Cu_2(im)\subset A']^{3+}$ (1)). To 1.0 mL of a 10 mM aqueous solution of $Cu(NO_3)_2 \cdot 2.5H_2O$ was added dropwise 0.5 mL of a 10 mM aqueous solution of A′, resulting in the immediate formation of a deep blue color. Imidazole (0.5 mL of a 10 mM aqueous solution) and NaOH (0.5 mL of a 10 mM aqueous solution) were added and the mixture was stirred for 15 min. The presence of the $[Cu_2(im)\subset A']^{3+}$ unit was confirmed by its characteristic ESR spectrum[7b,8b] (vide infra). Sodium thiocyanate (0.5 mL of a 1.0 M aqueous solution) was then added dropwise. Blue crystals grew rapidly from the solution. The unit cell determined by X-ray diffractometry and the density of these crystals showed them to be the same as $[Cu_2(NCS)_4\subset A']$ prepared by Method 2.

Method 2. To a methanolic solution of A′ (1.0 mL, 0.03 M) was added 1.0 mL of a 0.06 M methanolic solution of $Cu(NO_3)_2 \cdot 2.5H_2O$. The resulting deep blue solution was stirred for 5 min, and 1.0 mL of a 0.12 M aqueous KSCN solution was added. Upon standing, X-ray quality crystals, deep blue prisms, separated from the mixture. One of these crystals was used in the structural characterization of the complex reported below. Anal. Calcd for $Cu_2C_{22}H_{42}N_{10}S_4$: C, 37.64; H, 6.03; N, 19.95. Found: C, 37.98; H, 6.22; N, 20.03. IR in Nujol mull: ν_{CN} 2055, 2090 cm^{-1}; ν_{CS} 712, 752 cm^{-1}. UV–vis: λ_{max} = 600, 270 nm.

$[Cu_2(NCS)_2\subset A'](ClO_4)_2 \cdot 2H_2O$ (3). Deep blue needles of this compound were obtained by treating $[Cu_2(im)\subset A'](ClO_4)_3 \cdot H_2O$[7b,8a] with excess potassium thiocyanate in hot water followed by slow cooling.

(11) Martin, A. E.; Bulkowski, J. E. *J. Org. Chem.* **1982**, *47*, 415.
(12) Bolton, J. R.; Borg, D. C.; Swartz, H. M. In "Biological Applications of Electron Spin Resonance", Swartz, H. M.; Bolton, J. R.; Borg, D. C., Eds.; Wiley-Interscience: New York, 1972; p 100.

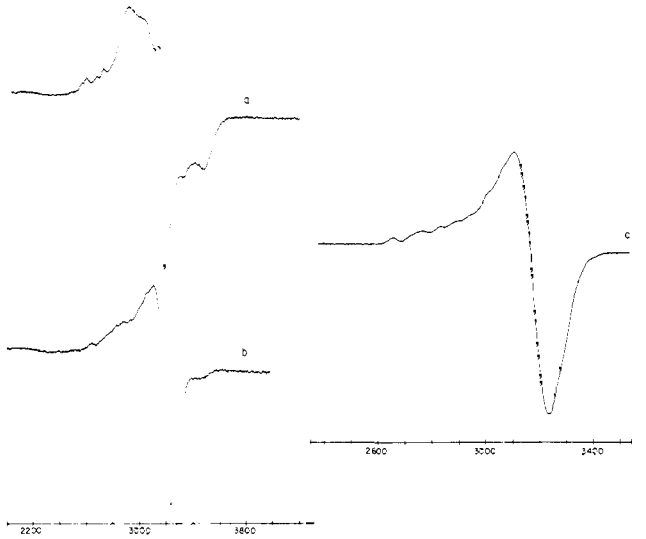

Figure 1. Electron spin resonance spectra in 50% aqueous (pH ~6) dimethyl sulfoxide of frozen solutions at 140 K of (a) $[Cu_2(im)\subset A']^{3+}$ (**1**), 1 mM; (b) sample as in (a) but containing a 10-fold excess of NaSCN; (c) $[Cu_2(NCS)_4\subset A']$ (**2**). For (a) and (b) the microwave power was 20 mW and the scan range was 4 kG. For (c) the microwave power was 12.5 mW and the scan range, 2 kG. The microwave frequency was 9.124 GHz.

Single-crystal X-ray studies revealed a monoclinic cell a = 14.339 (2) Å, b = 18.939 (2) Å, c = 6.515 (4) Å, β = 104.84 (2)°, ρ_{obsd} = 1.594 g cm^{-3}, ρ_{calcd} = 1.594 g cm^{-3} for Z = 2 of the above formula. A partial structure solution of this material confirmed the existence of the $[Cu_2(NCS)_2\subset A']^{2+}$ cation (vide infra).

Collection and Reduction of X-ray Data for $[Cu_2(NCS)_4\subset A']$ (2). The crystal used for the diffraction study was a dark blue prism bounded by (100) and ($\bar{1}00$), 0.22 mm apart, (001) and (00$\bar{1}$), 0.42 mm apart, and (021) and (0$\bar{2}\bar{1}$), 0.46 mm apart. Study on the diffractometer showed that the crystal belonged to the monoclinic system. Its quality was checked by taking open-counter ω scans of several low-angle reflections and was judged to be acceptable ($\Delta\bar{\omega}_{1/2} \approx 0.15°$). The diffractometer output revealed extinctions consistent with space group $P2_1/c$ (C_{2h}^5, No. 14).[13] Details of the data collection and reduction are given in Table I.

Determination and Refinement of the Structure. The positions of the copper atoms were obtained by using the direct methods program of SHELX-76.[14] Subsequent difference Fourier maps revealed the remaining non-hydrogen atoms, all of which were assigned anisotropic thermal parameters in the final refinement. Hydrogen atoms were allowed to refine as fixed methylene groups (C–H = 0.95 Å), with each group having an individual isotropic temperature factor. For five of the eighteen groups, this factor was fixed; for the remaining groups it was allowed to refine. Hydrogen atoms on the nitrogen atoms were assigned a common, fixed isotropic temperature factor.

The residual indices[15] converged at R_1 = 0.052 and R_2 = 0.064. The function minimized in the least-squares refinement was $\sum w(|F_o| - |F_c|)^2$, where $w = 2.5848/[\sigma^2(F_o) + 0.00046F_o^2]$. Neutral atom scattering factors were taken from ref 16. In the final cycle of refinement, no variable shifted by more than 0.02 σ (most by less than 0.005 σ) except for the five fixed isotropic methylene groups, which shifted by 0.12 σ. The largest peak on the final difference Fourier map was 0.85 e Å^{-3} located 1.34 Å from atom C(17). All remaining peaks were less than 0.72 e Å^{-3}.

Results and Discussion

Synthetic and Electron Spin Resonance Studies. Figure 1a shows the frozen solution spectrum of a 1 mM solution of macrocycle

(13) "International Tables for X-ray Crystallography", 3rd ed.; Kynoch Press: Birmingham, England, 1973; Vol. I., p 99.
(14) All calculations were performed on a DEC VAX-11/780 computer using SHELX-76: Sheldrick, G. M. In "Computing in Crystallography"; Schenk, H.; Olthof-Hazekamp, R.; van Koningsveld, H.; Bassi, G. C., Eds.; Delft University Press: Delft, The Netherlands, 1978; pp 35–42.
(15) $R_1 = \sum||F_o| - |F_c||/\sum|F_o|$; $R_2 = [\sum w(|F_o| - |F_c|)^2/\sum w|F_o|^2]^{1/2}$.
(16) "International Tables for X-ray Crystallography"; Kynoch Press: Birmingham, England, 1974; Vol. IV, pp 99, 149.

Table II. Final Positional Parameters for $[Cu_2(NCS)_4 \subset A']$ (2)[a]

atom	x	y	z
Cu1	0.76817 (4)	0.15353 (4)	0.82719 (4)
Cu2	0.20959 (4)	0.14849 (4)	0.68522 (4)
S41	1.07605 (12)	0.32152 (13)	0.86556 (13)
C41	0.9859 (4)	0.2512 (4)	0.8580 (3)
N41	0.9216 (3)	0.2040 (4)	0.8518 (3)
S51	0.37164 (14)	0.39080 (13)	0.61278 (15)
C51	0.3108 (4)	0.3129 (4)	0.6402 (3)
N51	0.2684 (4)	0.2570 (3)	0.6595 (3)
N1	0.7509 (3)	0.0816 (3)	0.7162 (3)
C2	0.7871 (4)	−0.0145 (4)	0.7409 (4)
C3	0.8632 (4)	−0.0155 (4)	0.8350 (4)
N4	0.8150 (3)	0.0316 (3)	0.8864 (3)
C5	0.8760 (4)	0.0523 (4)	0.9803 (4)
C6	0.8152 (4)	0.1129 (4)	1.0116 (3)
N7	0.7790 (3)	0.1927 (3)	0.9510 (3)
C8	0.6919 (4)	0.2392 (4)	0.9562 (4)
C9	0.5963 (3)	0.1854 (4)	0.9121 (3)
C10	0.5067 (3)	0.2344 (4)	0.9138 (4)
C11	0.4127 (3)	0.1801 (4)	0.8718 (4)
C12	0.3201 (3)	0.2331 (4)	0.8648 (4)
N13	0.2262 (3)	0.1871 (3)	0.8094 (3)
C14	0.2021 (4)	0.1073 (4)	0.8527 (4)
C15	0.1278 (4)	0.0471 (4)	0.7844 (4)
N16	0.1716 (3)	0.0294 (3)	0.7188 (3)
C17	0.1148 (5)	−0.0220 (5)	0.6405 (5)
C18	0.1690 (4)	−0.0190 (4)	0.5824 (4)
N19	0.1980 (3)	0.0774 (3)	0.5740 (3)
C20	0.2826 (3)	0.0843 (5)	0.5469 (3)
C21	0.3820 (3)	0.0586 (4)	0.6200 (3)
C22	0.4669 (3)	0.0814 (5)	0.5937 (4)
C23	0.5678 (3)	0.0599 (4)	0.6662 (3)
C24	0.6525 (3)	0.0859 (4)	0.6402 (3)
S61	0.02676 (11)	0.22650 (12)	0.59570 (11)
C61	−0.0605 (4)	0.1730 (4)	0.6154 (3)
N61	−0.1217 (4)	0.1347 (5)	0.6252 (4)
S31	0.63100 (12)	0.40479 (13)	0.64242 (12)
C31	0.6703 (4)	0.3208 (4)	0.7144 (4)
N31	0.6979 (3)	0.2631 (4)	0.7650 (3)

[a] Atoms are labeled as shown in Figure 2. Estimated standard deviations in the last significant digit(s) are given in parentheses.

A′ to which has been added 2 equiv of cupric nitrate and 1 equiv each of imidazole (imH) and sodium hydroxide. The high-field (~3450 G) "$g \sim 1.9$" feature present in this spectrum is characteristic of the $\{Cu_2(im)\}^{3+}$ unit.[6-8] The spectrum closely resembles that of $[Cu_2(im) \subset A'](ClO_4)_3 \cdot H_2O$.[3,8b] Upon the addition of a 10-fold excess of sodium thiocyanate (Figure 1b) the high-field feature has nearly vanished, a result similar to that observed when dissolved $[Cu_2(im) \subset A'](ClO_4)_3 \cdot H_2O$ was allowed to react with excess thiocyanate ion.[8] The most straightforward interpretation of these ESR spectral changes is that excess thiocyanate cleaves the imidazolate bridge, forming a copper(II) thiocyanate complex of the binucleating macrocycle. Alternatively, thiocyanate might form an adduct, "$[Cu_2(im)(SCN)_2 \subset A']^{+}$", in which, unlike $[Cu_2(im)(imH)_2 \subset A']^{3+}$,[8b] the unpaired electron on each of the copper(II) centers no longer occupies an orbital directed at the nitrogen atoms of the bridging imidazolate ligand. In such a case the spin-exchange interaction could be quite small, and the ESR spectrum would no longer resemble that of a coupled binuclear system. In order to evaluate this possibility, the thiocyanate adduct was isolated and its crystal structure determined. As shown in Figure 1c, the ESR spectrum of this well-characterized compound, **2**, is nearly the same as that in Figure 1b, confirming that a bridge-splitting reaction did indeed occur.

Treatment of a solution of the known compound $[Cu_2(im) \subset A'](ClO_4)_3 \cdot H_2O$ with excess thiocyanate also gave a crystalline product, $[Cu_2(NCS)_2 \subset A'](ClO_4)_2 \cdot 2H_2O$. Although disorder and a superlattice prevented complete refinement, the structure was solved to the point ($R_1 = 0.22$)[15] where the unbridged cation $[Cu_2(NCS)_2 \subset A']^{2+}$ was clearly defined.

Structure of $[Cu_2(NCS)_4 \subset A']$ (2). The final atomic positional parameters with their estimated standard deviations for all nonhydrogen atoms are reported in Table II. Interatomic distances and angles are given in Table III. A listing of hydrogen positional parameters, thermal parameters for all atoms, and a summary of observed and calculated structure factors are available as supplementary material (Tables S1–S3).

Table III. Interatomic Distances (Å) and Angles (deg) for $[Cu_2(NCS)_4 \subset A']$ (2)[a]

Copper Coordination Sphere			
Cu(1)-N(1)	2.037 (4)	Cu(2)-N(13)	2.050 (4)
Cu(1)-N(4)	2.000 (4)	Cu(2)-N(16)	1.962 (4)
Cu(1)-N(7)	2.070 (4)	Cu(2)-N(19)	2.057 (4)
Cu(1)-N(31)	1.944 (5)	Cu(2)-N(51)	1.922 (5)
Cu(1)-N(41)	2.248 (4)	Cu(2)-S(61)	2.733 (2)
Cu(1)-Cu(2)	7.577 (1)		
N(1)-Cu(1)-N(4)	83.4 (2)	N(13)-Cu(2)-N(16)	83.5 (2)
N(1)-Cu(1)-N(7)	164.9 (2)	N(13)-Cu(2)-N(19)	165.7 (2)
N(1)-Cu(1)-N(31)	95.4 (2)	N(13)-Cu(2)-N(51)	96.9 (2)
N(1)-Cu(1)-N(41)	94.4 (2)	N(13)-Cu(2)-S(61)	97.0 (1)
N(4)-Cu(1)-N(7)	83.3 (2)	N(16)-Cu(2)-N(19)	83.4 (2)
N(4)-Cu(1)-N(31)	169.2 (2)	N(16)-Cu(2)-N(51)	170.6 (2)
N(4)-Cu(1)-N(41)	94.4 (2)	N(16)-Cu(2)-S(61)	100.7 (1)
N(7)-Cu(1)-N(31)	96.4 (2)	N(19)-Cu(2)-N(51)	95.2 (2)
N(7)-Cu(1)-N(41)	93.6 (2)	N(19)-Cu(2)-S(61)	90.9 (1)
N(31)-Cu(1)-N(41)	96.3 (2)	N(51)-Cu(2)-S(61)	88.6 (1)
Thiocyanate Geometry			
N(31)-C(31)	1.134 (7)	C(31)-S(31)	1.636 (6)
N(41)-C(41)	1.137 (6)	C(41)-S(41)	1.636 (6)
N(51)-C(51)	1.145 (7)	C(51)-S(51)	1.615 (6)
N(61)-C(61)	1.125 (7)	C(16)-S(61)	1.641 (6)
N(31)-C(31)-S(31)	179.3 (5)	Cu(1)-N(31)-C(31)	160.9 (5)
N(41)-C(41)-S(41)	178.3 (5)	Cu(1)-N(41)-C(41)	161.7 (5)
N(51)-C(51)-S(51)	179.2 (5)	Cu(2)-N(51)-C(51)	170.3 (5)
N(61)-C(61)-S(61)	176.9 (6)	Cu(2)-N(61)-C(61)	112.0 (2)
Macrocycle Geometry			
N(1)-C(2)	1.487 (7)	N(13)-C(14)	1.476 (7)
C(2)-C(3)	1.505 (7)	C(14)-C(15)	1.493 (8)
C(3)-N(4)	1.478 (6)	C(15)-N(16)	1.495 (7)
N(4)-C(5)	1.476 (6)	N(16)-C(17)	1.433 (7)
C(5)-C(6)	1.488 (7)	C(17)-C(18)	1.480 (9)
C(6)-N(7)	1.481 (7)	C(18)-N(19)	1.482 (8)
N(7)-C(8)	1.482 (6)	N(19)-C(20)	1.489 (6)
C(8)-C(9)	1.511 (7)	C(20)-C(21)	1.518 (6)
C(9)-C(10)	1.508 (6)	C(21)-C(22)	1.518 (7)
C(10)-C(11)	1.494 (7)	C(22)-C(23)	1.514 (7)
C(11)-C(12)	1.526 (6)	C(23)-C(24)	1.522 (7)
C(12)-N(13)	1.472 (6)	C(24)-N(1)	1.485 (6)
C(2)-N(1)-Cu(1)	109.2 (3)	C(12)-N(13)-Cu(2)	116.6 (3)
C(24)-N(1)-Cu(1)	117.7 (3)	C(14)-N(13)-Cu(2)	108.6 (3)
C(3)-N(4)-Cu(1)	105.9 (3)	C(15)-N(16)-Cu(2)	108.2 (4)
C(5)-N(4)-Cu(1)	106.2 (3)	C(17)-N(16)-Cu(2)	109.1 (4)
C(6)-N(7)-Cu(1)	108.7 (3)	C(18)-N(19)-Cu(2)	108.0 (3)
C(8)-N(7)-Cu(1)	117.5 (3)	C(20)-N(19)-Cu(2)	117.5 (3)
N(1)-C(2)-C(3)	109.1 (4)	N(13)-C(14)-C(15)	109.6 (4)
C(2)-C(3)-N(4)	105.3 (4)	C(14)-C(15)-N(16)	104.6 (4)
C(3)-N(4)-C(5)	118.2 (4)	C(15)-N(16)-C(17)	118.9 (5)
N(4)-C(5)-C(6)	107.0 (4)	N(16)-C(17)-C(18)	107.7 (5)
C(5)-C(6)-N(7)	109.0 (4)	C(17)-C(18)-N(19)	109.9 (5)
C(6)-N(7)-C(8)	113.3 (4)	C(18)-N(19)-C(20)	113.6 (4)
N(7)-C(8)-C(9)	113.3 (4)	N(19)-C(20)-C(21)	113.2 (4)
C(8)-C(9)-C(10)	113.5 (4)	C(20)-C(21)-C(22)	110.9 (4)
C(9)-C(10)-C(11)	113.3 (5)	C(21)-C(22)-C(23)	112.6 (5)
C(10)-C(11)-C(12)	113.6 (4)	C(22)-C(23)-C(24)	112.1 (5)
C(11)-C(12)-N(13)	113.8 (4)	C(23)-C(24)-N(1)	112.3 (4)
Nonbonding Contact			
S(31)···S(51)	3.651 (3)		

[a] See footnote *a*, Table II. Distances have not been corrected for thermal motion.

The structure of $[Cu_2(NCS)_4 \subset A']$ is presented in Figure 2. Within the macrocycle the two copper ions are noninteracting (Cu1–Cu2 = 7.577 (1) Å). Both coppers are in an approximately square-pyramidal environment, with the basal positions consisting of three nitrogen atoms of the diethylenetriamine fragment of the macrocycle and one nitrogen atom from a thiocyanate ligand. As previously observed for complexes of A′,[8] the copper–nitrogen distance to the central diethylenetriamine nitrogen is significantly shorter than for the other two nitrogens (Table III). A similar

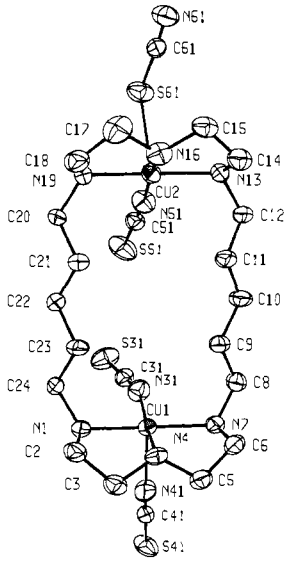

Figure 2. Structure of $[Cu_2(NCS)_4 \subset A']$ (**2**) showing the 40% probability thermal ellipsoids and atom-labeling scheme.

trend is observed for the analogous nonmacrocyclic complex, $[Cu(dien)(NCS)_2]$,[17] dien = diethylenetriamine. The shortest bonds in the basal planes of both coppers are to the thiocyanate ligands (Cu(1)–N(31) = 1.952 (6) Å, Cu(2)–N(51) = 1.928 (6) Å), as was also found for the dien complex (Cu–N = 1.97 Å).[17] A major difference in the basal coordination planes of the two copper atoms is that Cu(1)–N(31) is $\sim 4\sigma$ longer than Cu(2)–N(51). This result may be due to the effect of the different apical ligands. For Cu(1), a nitrogen-bound thiocyanate occupies the apical position (Cu(1)–N(41) = 2.240 (6) Å). By comparison, the axial Cu–N distance for $[Cu(dien)(NCS)_2]$ is 2.26 Å.[17] The coordination sphere of Cu(2), however, is completed by a weakly interacting, sulfur-bound thiocyanate ligand (Cu(2)–S(61), 2.733 (2) Å). The absence of a strongly bound axial ligand may be responsible for the contraction in the basal plane Cu(2)–N(51) and Cu(2)–N(16) bonds.

It is less common,[18] although not unprecedented,[19] for thiocyanate to bind copper(II) through the sulfur atom. Sulfur-bound thiocyanate is more usually associated with copper(I),[18] where it is even known to produce an S-monohapto-bridged binuclear structure.[20] The Cu(2)–S(61) bond length of 2.733 (2) Å and Cu(2)–S(61)–C(61) angle of 112.0 (2)° in **2** are both somewhat larger than the corresponding parameters, 2.607 (2) Å and 89.5 (1)°, in [Cu(trien)(SCN)](NCS).[19] Steric factors,[21] including packing interactions, and even solubility considerations[22] have been shown to be important in dictating the mode of thiocyanate–metal binding, and such may be the case for the weak, sulfur-bound thiocyanate ligand in **2**.

The internal geometry of the thiocyanate ligands is in accord with literature values for related compounds;[18,23] each of the four N–C–S bond angles is nearly linear (Table III). The S- and N-bonded thiocyanate ligands are clearly distinguished in the C–N stretching frequency region of the infrared spectrum of **2**. The higher frequency band may be assigned to the ligand weakly bonded to copper through a sulfur atom.[18]

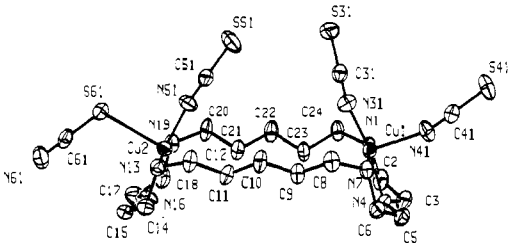

Figure 3. View of the structure of **2** depicting the extended linker chains of the binucleating macrocycle and the S···S van der Waals contact.

Macrocycle A′ has no unusual bond lengths or angles. It is in the fully extended, "planar", conformation with endo–endo puckering of all four of the ethylenediamine chelate rings (Figure 3).[24] The two thiocyanate ligands coordinated to the basal planes of the two copper centers have a nonbonded S···S contact of 3.65 Å and are thus in van der Waals contact.[25] The hydrophobic region in the center of the macrocycle is unoccupied by any bridging ligand. Space at the sixth coordination sites of the two copper centers is filled by the four methylene groups of the linker chains, C(9), C(11), C(21), and C(23) (Figure 2); the Cu–H distances for these methylene groups ranged from 2.80 to 2.87 Å.

Relevance to Cu_2Cu_2SOD. The ESR spectrum of the $[Cu_2(im)\subset A']^{3+}$ cation **1** undergoes a change in the presence of thiocyanate ion indicative of conversion of a magnetically coupled bimetallic system to isolated (noninteracting) copper centers. This change is similar to that observed for Cu_2Cu_2SOD.[3] Previously, the results for the protein were interpreted according to the following scheme:[3]

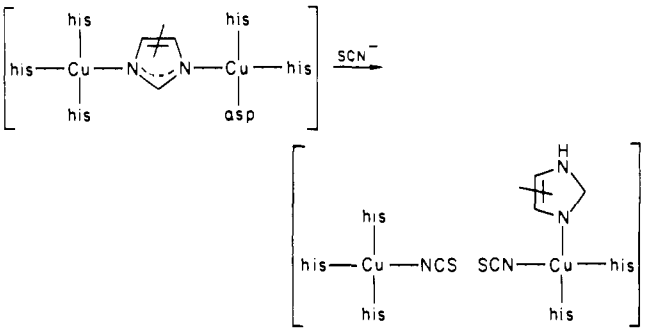

It was recognized, however, that thiocyanate might not have cleaved the bridge but rather, as discussed above, could have changed the orbital orientations enough to eliminate the magnetic coupling. The present work with the model complex $[Cu_2(im)\subset A']^{3+}$ supports the original interpretation. Treatment of the model compound **1** with thiocyanate cleaves the imidazolate bridge as shown by the structural determination of **2**. Moreover, it appears that the $\{Cu_2(im)\}^{3+}$ unit is inherently unstable in the presence of excess thiocyanate, both in the Cu_2Cu_2SOD and the model system $[Cu_2(im)\subset A']^{3+}$, and that bridge cleavage in the former is more a consequence of the coordination chemistry of copper than some special property of the protein.

Conclusions

This work demonstrates the value of having incorporated the imidazolate-bridged dicopper(II) unit into a binucleating macrocycle (A′) as a model for the histidine-bridged active site in Cu_2Cu_2SOD. The stability of the resulting complex, $[Cu_2(im)\subset A']^{3+}$, to hydrolytic bridge-cleavage reactions in water enabled us to prove that the ESR spectral changes occurring when excess thiocyanate is added to the model compound and, by analogy, to

(17) Cannes, M.; Carta, G.; Marongui, G. *J. Chem. Soc., Dalton Trans.* **1974**, 553.
(18) Norbury, A. H. *Adv. Inorg. Chem. Radiochem.* **1975**, *17*, 231.
(19) Marongui, G.; Lingafelter, E. C.; Paoletti, P. *Inorg. Chem.* **1969**, *8*, 2763.
(20) Nelson, S. M.; Esho, F. H.; Drew, M. G. B. *J. Chem. Soc., Chem. Commun.* **1981**, 388.
(21) (a) Basolo, F.; Baddley, W. H.; Burmeister, J. L. *Inorg. Chem.* **1964**, *3*, 1203. (b) Palenik, G.; Mathew, M.; Steffen, W. L.; Beran, G. *J. Am. Chem. Soc.* **1975**, *97*, 1059.
(22) Kidd, R. G.; Spinney, H. G. *J. Am. Chem. Soc.* **1981**, *103*, 4759 and references cited therein.
(23) Stults, B. R.; Day, R. O.; Marianelli, R. S.; Day, V. W. *Inorg. Chem.* **1979**, *18*, 1847.
(24) For a detailed discussion of the conformational properties of ligands A and A′, see: Coughlin, P. K.; Lippard, S. J. *J. Am. Chem. Soc.* **1984**, *106*, 2328.
(25) Pauling, L. "The Nature of the Chemical Bond", 3rd ed.; Cornell University Press: Ithaca, NY, 1960; p 260.

Cu_2Cu_2SOD are the result of an imidazolate bridge-splitting process. The fact that the thiocyanate adduct of Cu_2Cu_2SOD remains catalytically active as a superoxide dismutase implies that the bridge is not essential for the enzyme mechanism.[2] The compound $[Cu_2(SCN)_4 \subset A']$ is the latest member of a rapidly growing class of bimetallic complexes of binucleating macrocycles.[26] Further bioinorganic and organometallic studies of this new area of coordination chemistry will be of interest.

(26) (a) "Copper Coordination Chemistry: Biochemical and Inorganic Perspectives"; Karlin, K. D., Zubieta, J., Eds.; Adenine Press: New York, 1983: Martin, A. E., Lippard, S. J., p 395. (b) Nelson, S. M., p 331. (c) Agnus, Y. L., p 371. (d) Bulkowski, J. E., Summers, W. E., III. p 445. (e) Comarmond, J., Plumeré, P.; Lehn, J.-M.; Agnus, Y.; Louis, R.; Weiss, R.; Kahn, O.; Morgenstern-Badarau, I. *J. Am. Chem. Soc.* **1982**, *104*, 6330.

Acknowledgment. This work was supported by grants from the National Institute of General Medical Sciences (NIGMS), NIH, and the National Science Foundation. A.E.M. was the recipient of a National Research Service Award, GM 07956, from the NIGMS. We thank Mr. Joel Wirth for experimental assistance and Dr. L. S. Hollis for help with the crystallography.

Registry No. $\mathbf{1}(ClO_4)_3$, 76096-70-3; **2**, 89302-54-5; **3**, 89302-56-7; Cu_2Cu_2SOD, 9054-89-1.

Supplementary Material Available: Tables S1-S3 listing hydrogen atom positional parameters, thermal parameters for all the atoms, and observed and calculated structure factors for **2** (19 pages). Ordering information is given on any current masthead page.

Binuclear Molybdenum Carbonyls Bridged Both by Hydride and by Bidentate Phosphine Ligands. Crystal and Molecular Structures of Salts of $(\mu\text{-H})(\mu\text{-Ph}_2\text{P(CH}_2)_n\text{PPh}_2)\text{Mo}_2(\text{CO})_8^-$ (n = 1-4) and Their Reactions with Acids

Marcetta Y. Darensbourg,*[1a] Ramadan El Mehdawi,[1b] Terry J. Delord,[1c] Frank R. Fronczek,[1c] and Steven F. Watkins[1c]

Contribution from the Departments of Chemistry, Texas A&M University, College Station, Texas 77843, Tulane University, New Orleans, Louisiana 70118, and Louisiana State University, Baton Rouge, Louisiana 70803. *Received July 12, 1983*

Abstract: Reaction of Et_4N^+ and Ph_4P^+ salts of $\mu\text{-HMo}_2(CO)_{10}^-$ with bidentate phosphine ligands in refluxing THF yielded salts of $\mu\text{-HMo}_2(CO)_8(Ph_2P(CH_2)_nPPh_2)^-$, n = 1-4, designated as anions $\mathbf{1}^-$, $\mathbf{2}^-$, $\mathbf{3}^-$, and $\mathbf{4}^-$. X-ray crystal structure analyses for two of the new compounds were carried out, and the following parameters were obtained. $Ph_4P^+\mathbf{1}^-$: $P2_1/c$, Z = 4, a = 13.886 (6) Å, b = 18.545 (9) Å, c = 20.156 (6) Å, β = 91.03 (4)°, V = 5190 (4) Å^3, R = 0.0413 for 4402 reflections with $|F_o| \geq 3\sigma|F_o|$. $Et_4N^+\mathbf{4}^-$: $P\bar{1}$, Z = 2, a = 8.760 (2) Å, b = 13.940 (4) Å, c = 19.686 (4) Å, α = 105.75 (2)°, β = 93.59 (2)°, γ = 97.38 (2)°, V = 2282 (1) Å^3, R = 0.0471 for 4720 reflections with $|F_o| \geq 3\sigma|F_o|$. Anions $\mathbf{1}^-$ and $\mathbf{4}^-$ are bridged by both H^- and the bidentate ligands and show overall bent, staggered configurations with $P_1\text{-}Mo_1\text{-}Mo_2\text{-}P_2$ torsion angles of 21° for $\mathbf{1}^-$ and 42° for $\mathbf{4}^-$. Similar framework bends (the intersection angle of $(OC)_{ax}$-Mo vectors) of ca. 160° and similar $Mo_1\text{-}H\text{-}Mo_2$ angles of ca. 131° are observed for $\mathbf{1}^-$ and $\mathbf{4}^-$. The Mo···Mo separation in $\mathbf{1}^-$ is 3.4028 (8) Å and in $\mathbf{4}^-$ it is 3.4995 (8) Å. The distance between the P-donor atoms in $\mathbf{1}^-$ is 3.19 Å and in $\mathbf{4}^-$ it is 5.08 Å. In $\mathbf{4}^-$ the hydride bridge is directed into the area underneath the ligand bridge (the $(CH_2)_4$ unit), whereas in $\mathbf{1}^-$ the plane of the hydride bridge is roughly perpendicular to the P-CH_2-P bridge. The observed ligand substitution site selection was rationalized on the basis of the best match of bridge ligand donor site separation and intermetal ligand coordination site separation in the bent, staggered form of the parent $\mu\text{-HMo}_2(CO)_{10}^-$. A specific synthesis of the dibridged neutral bimetallics $(\mu\text{-Ph}_2\text{P(CH}_2)_n\text{PPh}_2)(\mu\text{-Ph}_2\text{P(CH}_2)_2\text{PPh}_2)\text{Mo}_2(CO)_8$ (n = 1, 2) and $(\mu\text{-Ph}_2\text{As(CH}_2)_2\text{AsPPh}_2)(\mu\text{-Ph}_2\text{P(CH}_2)_2\text{PPh}_2)\text{Mo}_2(CO)_8$ has been based on low-temperature protonation of $\mathbf{2}^-$ in the presence of other bidentate ligands.

The flexibility of the M-H-M bridge in the dimeric hydride anions $\mu\text{-HM}_2(CO)_{10}^-$ (M = Cr, Mo, W) and substituted analogues has been demonstrated in the variable configurations that are determined by M,[2,3] by counterion and crystal packing influences,[4-6] and by substituent ligands.[7,8] The structural possibilities are defined according to the linearity (or lack thereof) of the intersecting vectors $OC_{ax}\text{-M}\cdots\text{M-}CO_{ax}$ and the staggering or eclipsing of the two equatorial $M(CO)_4$ units (or $M(CO)_3L$ units) with respect to each other: linear, eclipsed; linear, staggered; bent, eclipsed; and bent, staggered. The last of these predominates by far in the known solid-state structures. The second most common is the linear, eclipsed form, which is observed for the Et_4N^+ salts of the all-carbonyl hydrides $\mu\text{-HM}_2(CO)_{10}^-$ (M = Cr,[9] Mo,[5] and W[10]). Thus far there are no known structures in the bent, eclipsed

(1) (a) Texas A&M University. (b) Tulane University. (c) Louisiana State University.
(2) Bau, R.; Teller, R. G.; Kirtley, S. W.; Koetzle, T. F. *Acc. Chem. Res.* **1979**, *12*, 176 and references therein.
(3) Teller, R.; Bau, R. G. *Struct. Bonding (Berlin)* **1982**, *44*, 1.
(4) Petersen, J. L.; Brown, R. K.; and Williams, J. M. *Inorg. Chem.* **1981**, *20*, 158.
(5) Petersen, J. L.; Masino, A.; Stewart, R. P., Jr. *J. Organomet. Chem.* **1981**, *208*, 55.
(6) Roziere, J.; Teulon, P.; Grillone, M. D. *Inorg. Chem.* **1983**, *22*, 557.
(7) Darensbourg, M. Y.; Atwood, J. L.; Burch, R. R., Jr.; Hunter, W. E.; Walker, N. *J. Am. Chem. Soc.* **1979**, *101*, 2631.
(8) Darensbourg, M. Y.; Atwood, J. L.; Hunter, W. E.; Burch, R. R., Jr. *J. Am. Chem. Soc.* **1980**, *102*, 3290.
(9) Roziere, J.; Williams, J. M.; Stewart, R. P., Jr.; Petersen, J. L.; Dahl, L. F. *J. Am. Chem. Soc.* **1977**, *99*, 4497.

0002-7863/84/1506-2583$01.50/0